

RESEARCH

Open Access



Inferring transcriptomic dynamics implicated in odor fatty acid accumulation in adipose tissue of Hulun Buir sheep from birth to market

Yechan Zhao^{1,2}, Zhangyan Li³, Huimin Ou¹, Zhiliang Tan^{1,2} and Jinzhen Jiao^{1,2*}

Abstract

This study aimed to investigate the temporal accumulation of odor fatty acids (OFAs) in the dorsal subcutaneous adipose tissue, and uncover their dynamic regulatory metabolic pathways from the transcriptomic perspective in lambs from birth to market. Thirty-two Hulun Buir lambs were selected and randomly assigned to four different sampling stages following their growth trajectories: neonatal (day 1), weaning (day 75), mid-fattening (day 150), and late-fattening (day 180) stages. Results indicated that the contents of three OFAs increased progressively as lambs matured, with the most drastic change occurred at mid-fattening vs. weaning. The dynamic transcriptomic profiles exhibited two distinct phases, with differentially expressed genes (DEGs) before weaning were involved in immune homeostasis, whereas those after weaning were associated with nutrient metabolism. Furthermore, DEGs involved in lipid metabolism and branch-chain amino acid degradation pathways exhibited surge in expression at mid-fattening vs. weaning, with acetyl-CoA and branched-chain-CoA as intermediates, and driven by regulation of PPAR and AMPK signaling pathways. Overall, our findings provided novel insight into the critical time window and pivotal candidate genes of OFA synthesis in the adipose tissue, which will assist with the targeted development of nutritional strategies to inhibit OFA accumulation of lambs.

Keywords Lamb meat, Odor fatty acids, Dynamic accumulation, Adipose transcriptome, From birth to market

Introduction

Lamb meat, as a high-quality protein source, supplies humans with essential amino acids, vitamins and trace minerals [1]. A 100 g serving meets over half the human daily requirement for B vitamins, iron, and zinc [2]. Consumers favor lamb meat (the meat from lambs under one year of age) over mutton (the meat from sheep older than one year) due to its better eating quality [3]. In general, the eating quality of meat is described in terms of sensorial properties such as flavor, tenderness, and juiciness, which are important drivers for repeating consumer purchasing behavior [4].

*Correspondence:

Jinzhen Jiao
jjz@isa.ac.cn

¹CAS Key Laboratory of Agroecological Processes in Subtropical Region, Institute of Subtropical Agriculture, Chinese Academy of Sciences, Changsha, Hunan 410125, China

²University of the Chinese Academy of Sciences, Beijing 100193, China

³Laboratory of Animal Nutrition and Human Health, College of Life Sciences, Hunan Normal University, Changsha, Hunan 410081, China



© The Author(s) 2024. **Open Access** This article is licensed under a Creative Commons Attribution-NonCommercial-NoDerivatives 4.0 International License, which permits any non-commercial use, sharing, distribution and reproduction in any medium or format, as long as you give appropriate credit to the original author(s) and the source, provide a link to the Creative Commons licence, and indicate if you modified the licensed material. You do not have permission under this licence to share adapted material derived from this article or parts of it. The images or other third party material in this article are included in the article's Creative Commons licence, unless indicated otherwise in a credit line to the material. If material is not included in the article's Creative Commons licence and your intended use is not permitted by statutory regulation or exceeds the permitted use, you will need to obtain permission directly from the copyright holder. To view a copy of this licence, visit <http://creativecommons.org/licenses/by-nc-nd/4.0/>.

The characteristic “mutton” flavor, which deters some consumers [5], is attributed to three volatile branched-chain fatty acids (BCFAs): 4-methyloctanoic acid (MOA), 4-ethyl-octanoic acid (EOA), and 4-methylnonanoic acid (MNA), collectively termed odor fatty acids (OFAs) [6]. The OFAs accumulate in lambs’ adipose tissue at low $\mu\text{g/g}$ levels, challenging their quantification [7]. Minor variations in OFAs significantly impact mutton flavor and are influenced by factors like age, breed, and diet [8–10]. On this premise, inhibiting the accumulation of OFAs in the subcutaneous adipose tissue of lambs is vital to improving lamb meat’s market competitiveness. The first step toward achieving this goal would be to clarify the accumulation dynamics of OFAs in lambs from birth to market.

During the growth of livestock animals, lipid metabolism plays a critical role in influencing the quality and nutritional values of meat, which are characterized by fatty acid composition and fat deposition amount in various parts of the carcass [11]. In contrast to grazing diets, indoor feeding promotes expression of genes involved in lipid transport, leading to higher intramuscular fat content and peculiar volatile compound profile in the muscle of lambs [12]. Moreover, transcriptomic profile of goat kids’ muscles demonstrated that the expression of genes involved in *de novo* lipogenesis was greater from birth to weaning, and genes involved in fatty acid elongation and desaturation increased from weaning to day 90 [13]. As mentioned above, the function of OFAs as volatile BCFAs, and their accumulation pattern might be linked

to lipid metabolism [14]. However, the exact reactions associated with the biosynthesis of OFAs and the molecular mechanisms involved in the regulation of their accumulation are not systematically deciphered.

From lambs’ birth to market, the lambs undergo several growth stages, including neonatal, weaning and fattening stages, during which the process of fat accumulation is complex and unclear [15]. To fill the knowledge gap, this study was conducted to clarify the accumulation pattern of OFAs in the subcutaneous adipose tissue of lambs from birth to market, with emphasis on gene expression dynamics and functional alterations. Ultimately, this study may offer valuable insights to guide future research toward pinpointing the vital window period for mitigating OFA accumulation and formulating tailored strategies.

Materials and methods

Animals

The study was approved by the Animal Care and Use Committee, Institute of Subtropical Agriculture, Chinese Academy of Sciences, Changsha, China, with approval number ISA2021008. Thirty-two healthy newborn Hulan Buir lambs with similar birth weights (3.63 ± 0.46 kg) were used in this study. These lambs were randomly assigned to four sampling periods throughout their growth trajectory: neonatal, weaning, mid-fattening, and late-fattening stages, with eight replicates per group (half male and half female). Except for the neonatal stage, lambs from other groups lived with their dams and suckled freely from birth to day 42. Solid starter was supplied to the lambs from day 42 until weaning at day 60. Subsequently, lambs were housed in individual well-ventilated pens, and fed with solid starters from day 60 to 90, followed by a fattening diet from day 90 to the end of the experiment (day 180). Lambs were fed the appropriate stage of total mixed diets (Table 1) twice daily at 8:00 and 16:00, with free access to clean water.

Sample collection

Lambs from neonatal, weaning, mid-fattening, and late-fattening stages were humanely euthanized at the age of day 1, day 75, day 150, and day 180. All lambs were deeply anesthetized by intravenous administration of 3% pentobarbital sodium (30 mg/kg; Sigma, P3761, U.S.A.), and sacrificed by exsanguination. The dorsal subcutaneous adipose tissue samples were collected from back fat at the same site (above the back muscles between 12th to 13th ribs of right carcass side) from all lambs. Adipose tissue samples (approximately 1.5 g) were collected, wrapped in aluminum foil, snap-frozen in liquid nitrogen and stored at -80°C prior to RNA extraction. Additional 10 g of adipose tissue samples (3 g for neonatal lamb) were taken

Table 1 Composition and nutrient levels of solid starter and fattening diet (% DM basis)

Items	Solid starter ³	Fattening diet ³
Ingredients		
Alfalfa	10.00	40.00
Corn	46.00	32.00
Wheat bran	15.00	8.20
Soybean meal	24.70	15.80
CaCO ₃	1.30	0.50
CaHPO ₄	0.50	1.00
NaCl	0.50	0.50
Premix ¹	2.00	2.00
Total	100.00	100.00
Nutrient levels ²		
ME/(MJ/kg)	10.60	9.58
CP	18.44	16.90
NDF	16.74	26.62
ADF	10.23	19.39

¹Per kilogram premix contained the following: FeSO₄·H₂O 5,000 mg, CuSO₄·5H₂O 1,984 mg, ZnSO₄·H₂O 7,042 mg, MnSO₄·H₂O 5,084 mg, KIO₃ 150 mg, CoCl₂ 35 mg, NaSeO₃ 30 mg, VA 100,000 IU, VD 24,000 IU

²ME was a calculated value, while the others were measured values

³Lambs from weaning were fed by solid starter, and lambs from mid-fattening and late-fattening were fed by fattening diet

and vacuum-packed in sealable polyamide bags, stored at -20°C until determining the contents of OFAs.

Determination of three odor fatty acids

The MOA, MNA, and EOA, with a purity of $>98\%$, were purchased from Sigma Aldrich (Milwaukee, WI, USA), and used for preparation of standard samples. Before determination, the raw samples were freeze-dried for 48 h, grounded into powder, and then homogenized at room temperature. Lipids were extracted using the Soxhlet extraction method from 5 g of freeze-dried adipose tissue samples using the Soxhlet extraction method, employing a fully automated fat analyzer SOX416 (Gerhardt, Königswinter, Germany). After the solvent evaporated, acid-alkali derivatization method was applied to form fatty acid methyl esters, using two types of methylation reagents: 2% NaOH-CH₃OH and 0.5 mol/L H₂SO₄-CH₃OH, modified from the previous method by GG Hewavitharana, DN Perera, SB Navaratne and I Wickramasinghe [16]. These fatty acid methyl esters were then detected by gas chromatography-mass spectrometry (GC-MS 7890 A-5975 C, Agilent Technologies Inc, USA), equipped with a SP-2560 chromatographic column (100 m \times 0.25 mm \times 0.2 μm , Supelco, Bellefonte, USA). The contents of each OFAs in the adipose tissues were calculated from chromatograph peak areas using calibration with external standards of MOA, MNA, and EOA.

RNA extraction and sequencing

Total RNA was extracted from frozen samples using Trizol reagent (Invitrogen, CA, USA), then treated with DNase I to remove the remaining DNA. Qualitative and quantitative assessments of total RNA were performed following our previous workflow [17]. Afterwards, qualified RNAs were used to construct transcriptomic libraries through the following processes [13]: (1) purifying mRNA with magnetic beads with Oligo (dT); (2) breaking mRNA into short fragments; (3) synthesizing first-strand cDNA using mRNA fragmentation as templates, and then synthesizing second-strand cDNA; (4) repairing the ends, then adding A and adaptor ligation; (5) amplifying the products through polymerase chain reaction. Afterwards, libraries were sequenced on the BGISEQ-500 platform (Beijing Genomics Institute, Shenzhen, China) to obtain 150 bp paired-end reads.

Transcriptomic analysis

Raw sequencing data was filtered with SOAP nuke (v1.5.6) to obtain clean data [18]. The HISAT2 (v2.1.0) and Bowtie2 (v2.3.4.3) were applied to map clean reads to the *Ovis aries* genome (GCF_016772045.1_ARS-UI_Ramb_v2.0) and align to the known coding gene sets [19, 20]. Gene expression level was calculated and

normalized as fragments per kilobase transcript length per million mapped reads (FPKM) by RSEM (v1.3.1) [21].

Differential expression analysis was performed using the DESeq2 package (v1.4.5) of R software [20]. The temporal effect on mRNA expression was examined by performing the following consecutive comparisons: weaning vs. neonatal, mid-fattening vs. weaning, and late-fattening vs. mid-fattening. Differentially expressed genes (DEGs) were declared with thresholds of false discovery rate (FDR) of <0.05 and absolute \log_2 fold change >1.5 . The GO and KEGG enrichment analyses were performed by Phyper based on the Hypergeometric test. The significant levels of terms and pathways were selected at $\text{FDR} < 0.05$ [22].

Weighted gene co-expression network analysis

The WGCNA package (v1.47) of R software was used to construct the co-expression networks [23]. Sample clustering using the 'hclust' function was utilized to eliminate any sample outliers based on all gene expressions of each sample. Then using 'thePickSoftThreshold' function to select the parameter of soft thresholding power as 9, which could ensure scale-free topology and effective connectivity. Afterward, the hierarchical clustering was performed to compute gene expression distance for module detection using the 'blockwiseModules' function, with the parameters of min-module size as 20, module similarity threshold as 0.035, and the network type as unsigned, which identified 7 modules. Next, the module eigengene was computed by using the 'moduleEigengenes' function. Pearson's correlation-based associations between phenotypic traits (three odor fatty acids content) and module eigengene were calculated using the psych package (v 2.3.9), which was displayed by heatmap drawing with the pheatmap package (v 1.0.12) of R software. Modules with absolute $r > 0.5$, and $P < 0.05$ were considered to have a significant correlation with phenotypic traits.

Validation of RNA expression by quantitative PCR

Eleven DEGs were selected for real time quantitative PCR (RT-qPCR) analysis. The process of synthesizing cDNA from 1 μg of total RNA was carried out utilizing the Prime-Script 1st Strand cDNA Synthesis Kit (TAKARA, Dalian, China). RT-qPCR was conducted using SYBR premix Ex Taq II detection Kit (TAKARA, Dalian, China) on a lightcycler 480 II Sequence Detection System (Roche, Basel, Switzerland), as detailed in our previous study [17]. All primers were designed using Primer 5.0 software and validated for primer specificity and efficiency (Table 2). Relative gene expression values were standardized to the internal reference (β -actin and GADPH), determined by the $2^{-\Delta\Delta\text{Ct}}$ method.

Table 2 Genes and primers used for relative quantification by real time PCR

Gene name	Primer	Sequence (5'→3')	Length (bp)
β-actin ¹	Forward	TCCTGCCGCATTACGAAACTAC	80
	Reverse	GTGTTGGCGTAGAGGTCCTTGC	
GAPDH ¹	Forward	CGGCACAGTCAAGGCAGAGAAC	115
	Reverse	CACGTACTIONCAGCACCAGCATCAC	
ACACA	Forward	TTCGAAATGAGCGTGCGATC	71
	Reverse	GTATTCTGCGTTGGCTTTCAGG	
FASN	Forward	TTTGACGCTTCCTTCTTCGG	123
	Reverse	AATGGAAGCTGGGTTGATGC	
CPT1A	Forward	ACGGGAAAAACAAGCAGTGC	115
	Reverse	TAGCTGTCCATCGACGTTTCC	
FABP3	Forward	ACCAAGCCTACCACAATCATCG	150
	Reverse	TGTCACGATGGACTTGACCTTC	
ACADS	Forward	TCAAGATCGCCATGCAAACC	119
	Reverse	GAAAGCACTGCGGTTCTCAG	
HADH	Forward	AGTGTGGTGGATCAAACGG	126
	Reverse	TTCGCCACAAACTCATCAGC	
ALDH9A1	Forward	ATTGCCGAGATGACATGACC	108
	Reverse	TGGTGTCAATTGGCTCTTTCC	
BCKDHB	Forward	ATGAAGCTGCCAAGTATCCG	133
	Reverse	TGGGCAAAGAAAGCTTCAGG	
RXRG	Forward	AAGTGTGCAGGAAGAAAGG	118
	Reverse	ACAGCAAGTTCAGCTTCCAG	
PPARG	Forward	CCCAGGTTTCTGAATGTGAAG	126
	Reverse	ATTTTCTGAGCAGCTTGGC	
LIPE	Forward	GGCAAAAGTCCCACCTGAAATC	118
	Reverse	TTCAGGCTCTGAGGGAGTTG	

¹Housekeeping gene

Statistical analyses

Data of OFA content and gene expression of four growth stages were statistically analyzed using one-way analysis of variance (ANOVA) with Duncan’s t-test in SPSS (v 26.0, SPSS Inc., U.S.A.). Statistical significance was declared at $P < 0.05$.

Results

Odor fatty acid contents at different growth stages

The contents of the three OFAs in dorsal subcutaneous adipose tissue of Hulun Buir sheep varied substantially among four different growth stages ($P < 0.05$, Fig. 1). The

MOA and MNA contents exhibited a 5.3- and a 3.4-fold increase at late-fattening vs. mid-fattening, respectively, which consistently showed the highest increase rate at this period. Meanwhile, the EOA content exhibited a 9.1-fold increase at mid-fattening vs. weaning, and experienced another surge (41.5%) at late-fattening vs. mid-fattening.

Gene expression dynamics at different growth stages

After quality control and filtering, a total number of 1.19 billion clean reads with an average of 44.0 ± 1.2 million per sample were obtained. Through mapping to the ovine reference genome, 60.7% of reads were mapped to unique genome locations, and, 18,653 annotated genes were identified. Given that more than half of the genes exhibited an expression level of greater than 5 FPKM, a total of 9,778 genes with $FPKM > 5$ were selected for subsequent analysis.

As presented in Figs. 2A, 7,486 genes were commonly expressed in all growth stages, 390, 172, 192 and 137 genes were uniquely expressed in neonatal, weaning, mid-fattening, and late-fattening stages. Principal component analysis (PCA) showed distinct gene expression profiles among four growth stages (Fig. 2B). To investigate critical time windows and pivotal targets, we compared gene expression levels of groups at consecutive stages to identify DEGs (Fig. 2C). Among all comparisons, the comparison of mid-fattening vs. weaning has the highest number of DEGs (645 up-regulated; 527 down-regulated), followed by weaning vs. neonatal (379 up-regulated; 107 down-regulated) and late-fattening vs. mid-fattening (20 up-regulated; 145 down-regulated). Ultimately, we identified a total of 1,429 DEGs for further analysis.

The GO enrichment analysis showed these 1,429 DEGs were involved in the M band, structural constituent of muscle, fatty acid elongation, pointed-end actin filament capping, and lipoprotein particle binding (Fig. 2D). The top 20 significantly enriched KEGG pathways included fatty acid biosynthesis, steroid biosynthesis, 2-oxocarboxylic acid metabolism, and biosynthesis of amino acids (Fig. 2E). Of note, DEGs of weaning vs. neonatal involved

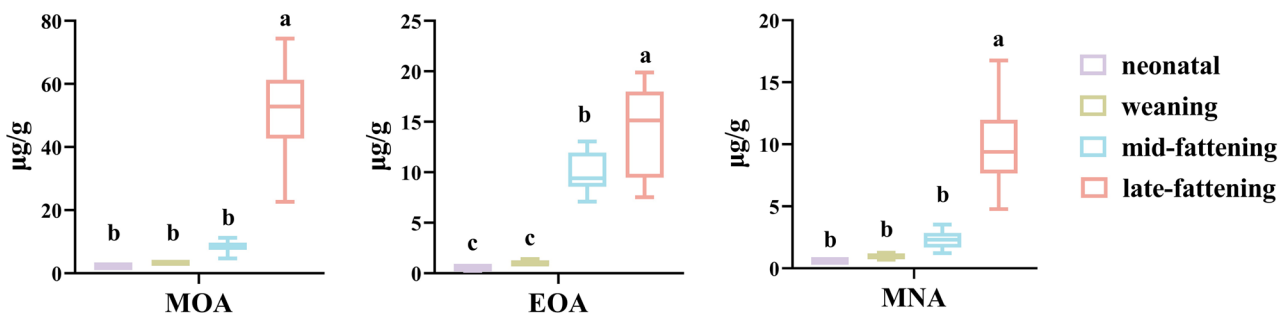


Fig. 1 Contents of odor fatty acids in dorsal subcutaneous adipose tissue of Hulun Buir sheep at different growth stages

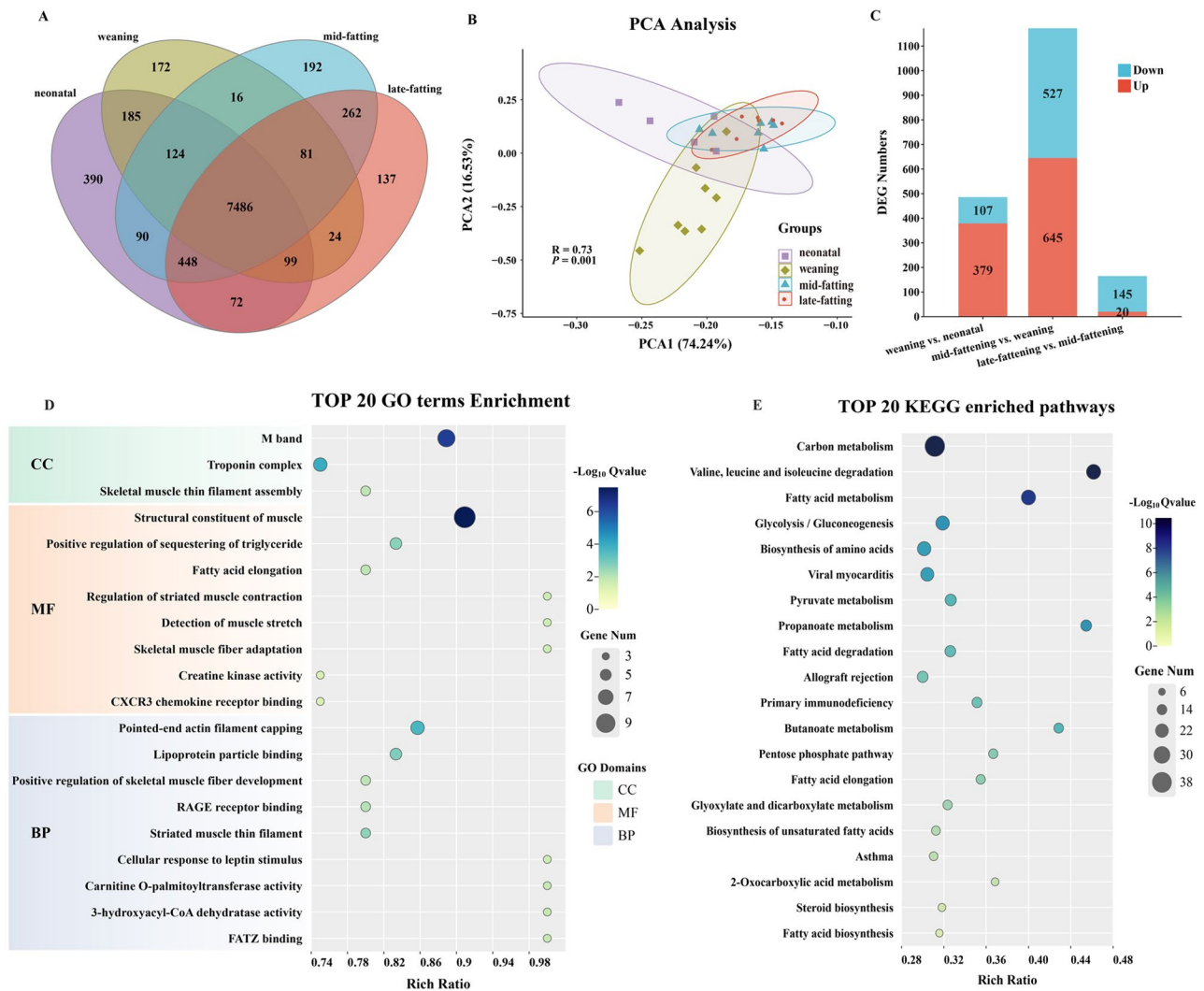


Fig. 2 Comparison of transcriptomes of subcutaneous adipose tissue between dorsal between different growth stages. **(A)** Venn diagram of the gene numbers among different growth stages. **(B)** Principal Component Analysis (PCA) plot for all of the samples based on the gene expression. **(C)** The numbers of DEGs between two consecutive growth stages. **(D)** The top 20 GO terms of all DEGs. **(E)** The top 20 KEGG-enriched pathways of all DEGs

in immune-related pathways, while DEGs of mid-fattening vs. weaning and late-fattening vs. mid-fattening were mainly involved in pathways related to metabolism and regulation of nutrients (Fig. S1).

Correlation between DEGs and the contents of OFAs

Weighted gene co-expression network analysis (WGCNA) was used to identify key genes affecting the contents of OFAs in DEGs. A total of 7 gene modules were finally identified by combining them into topology matrix based on gene expression (Fig. 3A). The modules ranged in size from 19 to 386. Three of these modules showed significant correlation with OFAs (Fig. 3B). Among them, M6 module (270 genes, 18.90% of DEGs) displayed a significantly positive correlation ($r > 0.5$, $P < 0.05$) with contents of all OFAs, while M7 module (270 genes, 18.90% of DEGs) showed a significantly

positive correlation ($r > 0.5$, $P < 0.05$) with contents of MOA and MNA. Major genes within these two modules showed higher expression during the mid-fattening and late-fattening stages (Fig. 3D and E). Furthermore, genes within M6 module were related to several lipid metabolism regulating pathways, such as regulation of lipolysis in adipocytes, AMPK, and PPAR signaling pathways (Fig. 3D). The genes contained in M7 module showed significant enrichment in fatty acid metabolism and valine, leucine and isoleucine degradation pathways, which are linked to branched-chain fatty acid biosynthesis (Fig. 3E). Conversely, M2 module demonstrates a significant negative correlation ($r < -0.5$, $P < 0.05$) with EOA. Genes within this module exhibited higher expression levels at the weaning and were involved in the biosynthesis of amino acids, gluconeogenesis, and pentose phosphate pathway (Fig. 3C).

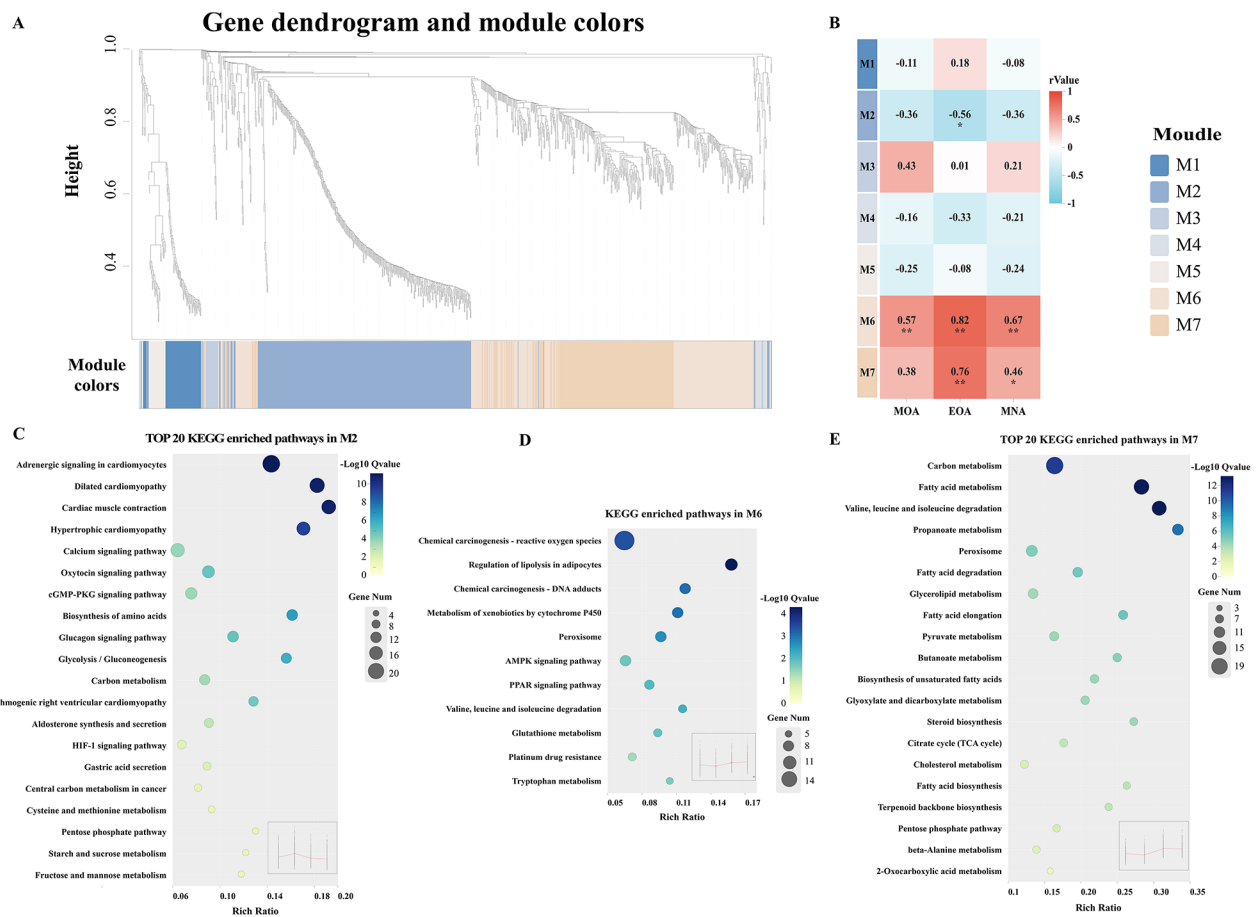


Fig. 3 The WGCNA analysis of all DEGs. (A) Co-expression dendrogram analysis subdivided into co-expressed modules. (B) The correlation between the transcriptome and phenotypic traits of sheep. The top 20 KEGG pathways in specific modules M2 (C), M6 (D), and M7 (E), and their expression profile

Lipid metabolism-related DEGs implicated in OFA accumulation

As mentioned above, DEGs exerted essential roles in lipid metabolism, especially the genes in the three modules significantly correlated with OFAs. Therefore, temporal changes of genes within those three modules were analyzed, with emphasis on several typical lipid metabolism pathways, including steroid synthesis, ketone synthesis, TAG synthesis, fatty acid synthesis, fatty acid transport, and fatty acid β -oxidation.

De novo lipogenesis is initiated from acetyl-CoA, which is carboxylated by acetyl-CoA carboxylase (*ACACA*, *ACSM1*, *ACSM3*) to form Mal-CoA. This is followed by the synthesis of fatty acid chains through the catalysis of fatty acid synthetase (*FASN*), and the extension of the carbon chain via a continuous cycle of 2 C unit condensation, ultimately forming palmitic acid (C16:0). Elongation and desaturation are catalysed by elongases (*HACD1*, *HACD2*, *HACD4*, *HSD17B12*, *DBI*, *ELOVL6*) and desaturase (*SCD*), respectively. The expression of these genes surged at mid-fattening, indicating that lambs synthesized substantial amounts of fatty acids including OFAs

at that stage (Fig. 4). Of note, *ACSM* and *HACD* exhibited individual expression patterns of such genes that differed from others because two or more isoenzymes were performing the same function. Free fatty acids are activated to R-SCoA by fatty acid coenzyme A ligase (*ACSL1*) in the cytoplasm, and transported to mitochondria with the assistance of fatty acid transporter proteins (*FABP5*, *FABP3*) and the carnitine acetyltransferase family (*CPT1A*). Expression of *ACSL1* surged in mid-fattening in accordance with changes in fatty acid synthesis-related enzymes. Remarkably, the expression of *FABP5*, *FABP3*, and *CPT1A* decreased after the weaning stage (Fig. 4A), which may indicate that large amounts of fatty acids influx into the adipocytes of neonatal and weaning lambs to supply energy for organism development.

Subsequently, energy is released through β -oxidation, which is catalysed by *ACADS*, *EHHADH*, and *HADH*. As expected, the expression of *ACADS*, and *HADH* was sharply increased at mid-fattening, implying that a large amount of energy required by lamb during this stage may be derived from the oxidation of fatty acids. R-SCoA participates in TAG biosynthesis in the cytoplasm, using

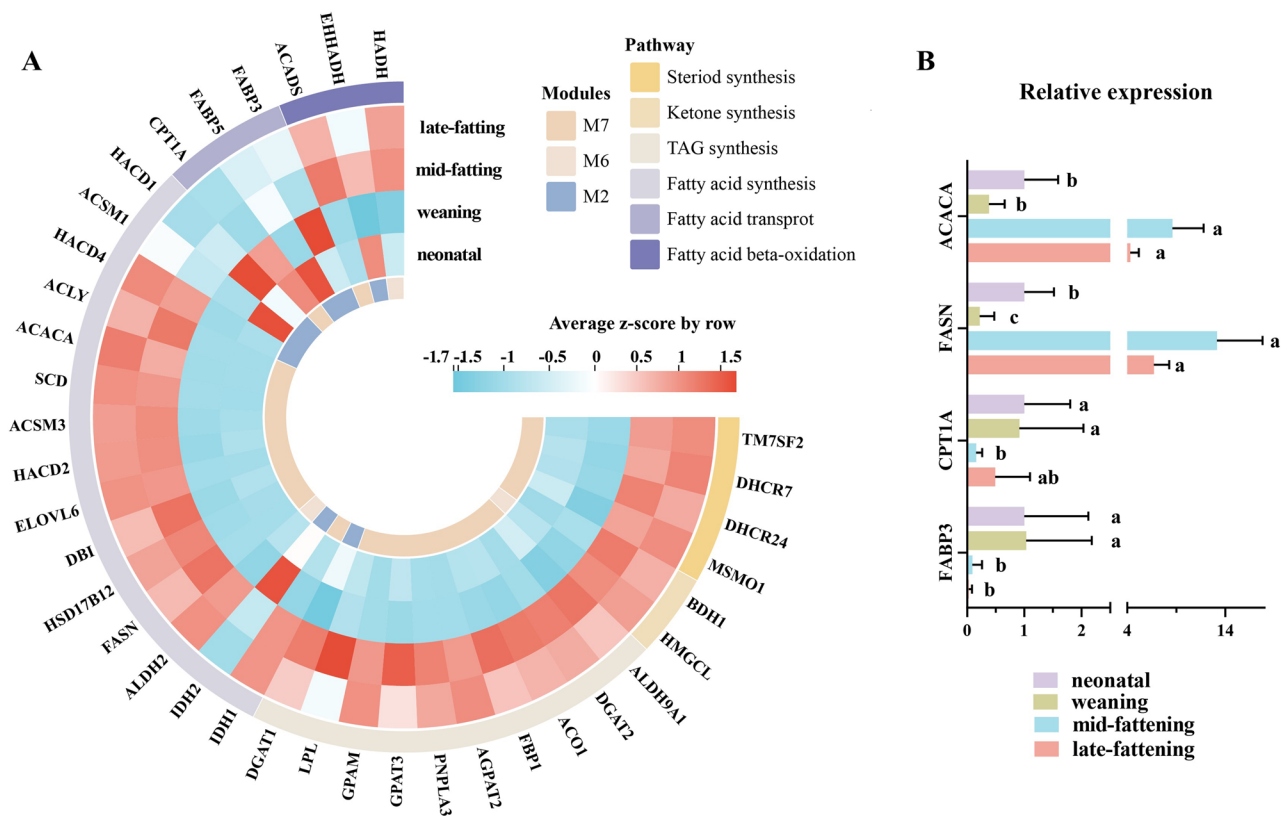


Fig. 4 Heatmap of genes involved in several typical lipid metabolism pathways. The expression of genes (FPKM) was normalized according to the z-score. Six typical lipid metabolism pathways (steroid synthesis, ketone synthesis, TAG synthesis, fatty acid synthesis, fatty acid transport, and fatty acid β -oxidation) are marked out in different colors (A). The relative gene expression from RT-qPCR (B)

glycerol-3-phosphate as a backbone, facilitated by glycolysis-related enzymes (*ALDH9A1*, *PNPLA3*), diacylglycerol acyltransferase (*DGAT1*, *DGAT2*), for energy storage in adipocyte lipid droplets. The expression of these genes exhibited changing patterns that increased after weaning (Fig. 4A). Meanwhile, the expression of extensive genes related to synthesis of ketones (*BDH1*, *HMGCL*) and steroids (*MSMO1*, *DHCR7*, *DHCR24*, and *TM7SF2*) from acetyl-CoA exhibited a parallel upward trend, indicating an increase in the function of these three pathways (Fig. 4A). RT-qPCR validation of partial genes (*ACACA*, *FASN*, *CPT1A*, *FABP3*) showed that expression change patterns were largely consistent with transcriptome (Fig. 4B).

BCAA metabolism-related DEGs implicated in OFA accumulation

Furthermore, genes in M6 played an essential role in the synthesis and accumulation of OFAs, and their KEGG enrichment pointed to the BCAA degradation pathway, which is closely linked to branched-chain fatty acid synthesis in adipose tissue. BCAAs undergo initial shared steps of transamination by branched-chain amino transferases (*BCAT2*) to form branched-chain α -ketoacids

(BCKAs), followed by oxidative decarboxylation with catalyzing by BCKDH complex (*BCKDHA*, *BCKDHB*, *DBT*) to produce branched-chain-CoA intermediates. A part of intermediates could cross the mitochondrial membrane with aid of carnitine O-acetyltransferase (*CRAT*), enter the cytoplasm, and subsequently act as a substrate for fatty acid synthesis in the presence of *FASN*. The expression of genes mentioned above increased as lambs matured, with 0.6-fold to 5.4-fold greater for fattening vs. weaning (Fig. 5A). Many critical genes (including *ACADA*, *ECHS1*, *ACSF3*) involved in catabolism of branched-chain-CoA intermediates through unique steps also surged in expression as lambs matured (Fig. 5A). RT-qPCR results also support the above change pattern (Fig. 5B).

DEGs involved in the PPAR and AMPK signaling pathways

Several signaling pathways were enriched, PPAR and AMPK in particular, which played a vital role in the regulation of lipid metabolism. The peroxisome proliferator-activated receptor γ (*PPAR γ*) binds to specific ligands, transferred to the nucleus, and heterodimerized with retinoid X receptor (*RXR γ*) to modify the expression of target genes involved in fatty acid transport and lipogenesis.

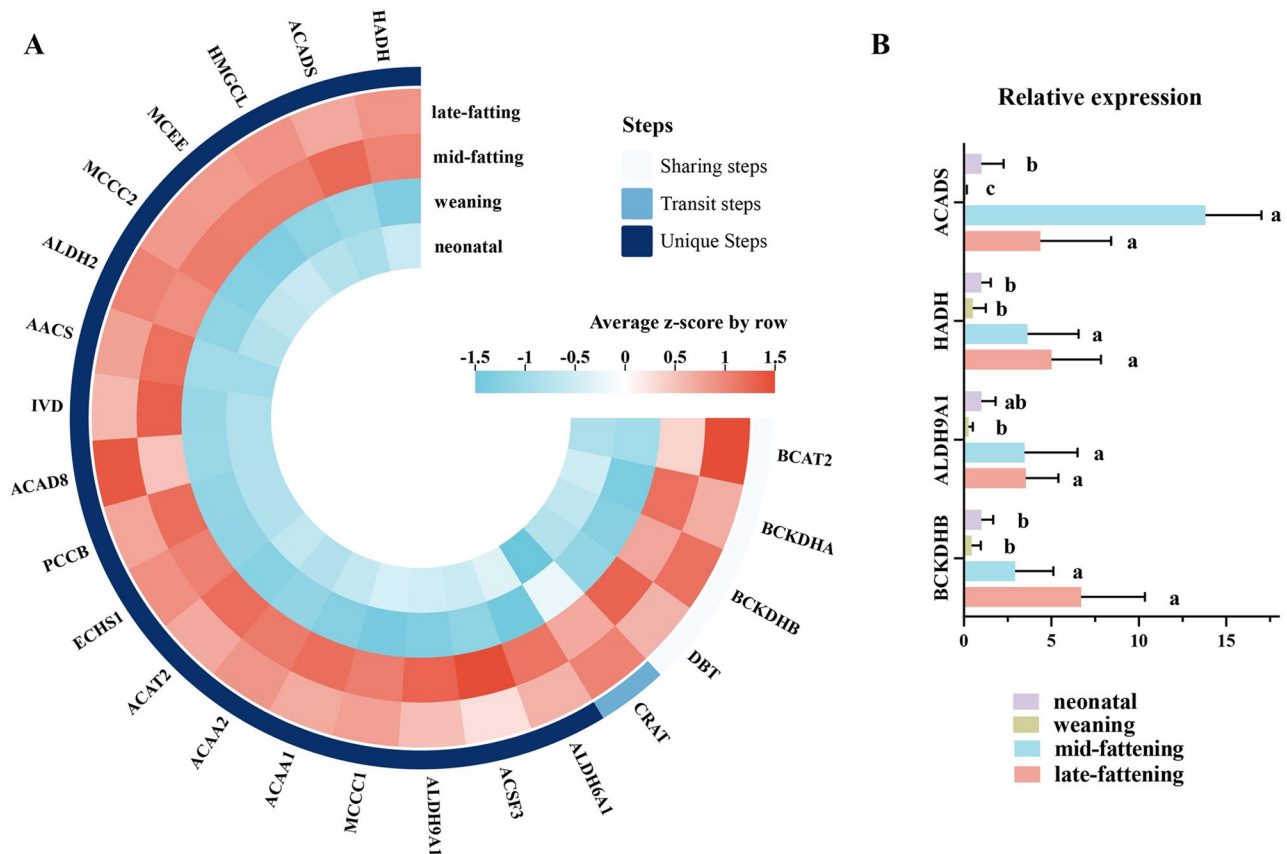


Fig. 5 Heat-map of genes involved in valine, leucine, and isoleucine degradation pathway. The expression of genes (FPKM) was normalized according to the z-score. The BCAA degradation pathway is classified into three types of steps (sharing steps, unique steps, and transit steps), which are marked with different colors (A). The relative gene expression from RT-qPCR (B)

Expression of *PPARγ* and *RXRG* were 3.3- and 3.9-fold greater at mid-fattening vs. weaning, respectively, whose expression shared a similar change pattern with target genes. The Amp-activated protein kinase (AMPK) inhibits the expression of genes implicated in lipid synthesis by phosphorylating sterol regulatory element binding protein-1 (*SREBF1*). Furthermore, AMPK can inhibit hormone-sensitive lipase (*LIPE*) by phosphorylating during lipolysis, while facilitating cellular uptake of fatty acids by upregulating *CD36* expression. Expression of *SREBF1* was 3.9-fold greater for mid-fattening vs. weaning, and expression of *LIPE* and *CD36* dropped by 67.3% and 64.7% during neonatal to weaning and then elevated over two-fold at fattening (Fig. 6A). Shifting patterns of gene expression are also evidenced in RT-qPCR (Fig. 6B).

Discussion

The three OFAs contributed greatly to the flavor of mutton due to their volatility, despite with minor or even undetectable levels in lambs. Generally, MOA content is roughly 3- to 10-fold greater than the other two OFAs, and MNA is the least abundant in the adipose tissues of lambs [7]. The accumulation of OFAs varies substantially

in different adipose tissues, with their amounts at subcutaneous adipose tissues greater than perirenal and mesenteric adipose tissues [24, 25], and hence we focused on the dorsal subcutaneous adipose tissue in the current study. Furthermore, RS Gravador, AP Moloney, NP Brunton, V Gkarane, P Allen, AG Fahey, NA Claffey, MG Diskin, LJ Farmer and FJ Monahan [26] found that MOA and MNA content in subcutaneous adipose of 293-day-old sheep was 3-fold greater than 196-day-old ones, implying that the accumulation of OFAs might be affected by the developmental ages of animals. On this premise, we clarify the accumulation dynamics of OFAs in lambs from birth to market and found that the most drastic change occurred at mid-fattening vs. weaning, which serves as the key time window for developing nutritional strategies to depress the accumulation of OFAs.

Adipose transcriptome is the complete mRNA expression collection of the tissue in response to internal or external factors, which can enhance the global insight into gene expression pattern and their regulatory mechanism [11]. In the current study, we identified a total of 1,429 DEGs among contiguous growth stages, suggesting dramatic temporal changes in the dorsal subcutaneous

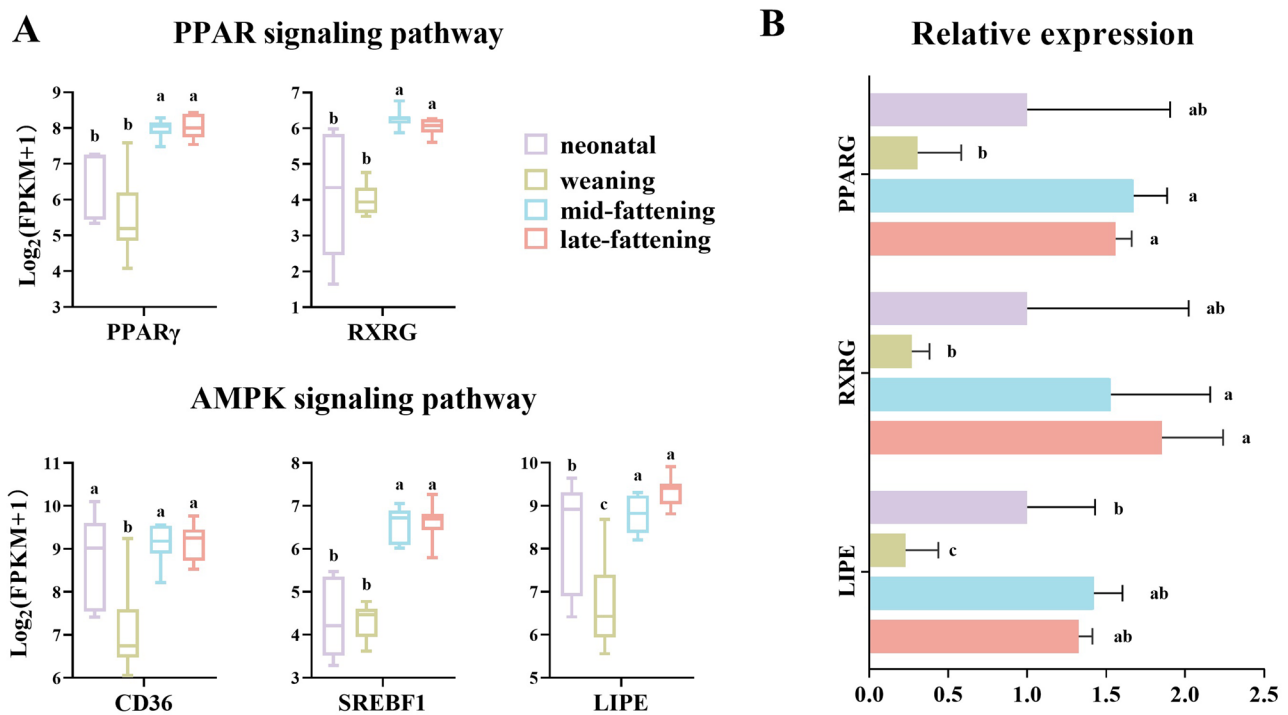


Fig. 6 The expression of genes involved in PPAR and AMPK signaling pathways at different growth stages (A). The relative gene expression from RT-qPCR (B)

adipose tissue during lamb development, in accordance with observations in sheep adipose tissue during the first month of life [27]. Of note, these DEGs played a vital role in immunity before weaning, whereas were mainly involved in metabolism-related pathways after weaning. This shifting law was consistent with findings in the muscle of goats [13], and rumen of sheep [28], suggesting that the shift from immune homeostasis establishment to nutrient metabolism is an intrinsic law during ruminant development, independent of the tissue type.

Insights from WGCNA analysis indicated that three modules significantly correlated with the content of OFAs, which were involved in lipid metabolism and BCAA degradation pathways, consistent with previous observations in the adipose tissue of yaks [29]. With a volatile odor due to their short carbon chains, OFAs are a category of C9 to C10 BCFAs with a methyl or ethyl chain branching point in the middle of the hydrocarbon chain [30]. Acetyl-CoA is a metabolite produced by the catabolism of glucose, fatty acids and amino acids (TCA cycle), which intersects with multiple pathways and represents a key intermediate in lipid metabolism that should not be ignored [31]. In order to understand the molecular mechanism of OFAs synthesis, it is important to investigate how branched-chain-CoA replaces acetyl-CoA as a precursor of fatty acid synthesis (Fig. 7). It is speculated that due to the promiscuity of *FASN*, branched-chain-CoA is used as the priming unit to initiate this repetitive

reaction [14], and methyl/ethyl group may crowd the limited enzyme binding channel space and induce premature termination of the synthesis of C16 palmitic acid with acetyl-CoA as substrate [32], thus releasing OFAs. As anticipated, expression of genes involved in lipid metabolism showed dramatic increases during the critical transition stage from weaning to mid-fattening, as the body accumulates large amounts of lipids, including OFAs. Among them, genes such as *ACACA*, *DGAT*, *FABP*, and *SCD* represent candidate genes affecting profile and accumulation of intramuscular fatty acids in sheep and cattle [12, 33, 34].

Additionally, it is well-recognized that BCAAs serve as important nutrient signals that directly or indirectly regulate a variety of biochemical functions such as lipid metabolism [35]. The branched-chain-CoA intermediates, which serve as key intermediates in the degradation of BCAAs and as important precursors for the *de novo* synthesis of BCAAs, including OFAs [36]. Furthermore, the subsequent breakdown products of branched-chain-CoA intermediates, propionyl-CoA and acetyl-CoA, also enter the TCA cycle to participate in lipid metabolism [14]. The expression patterns of *BCAT2* and *DBT* in this study surged sharply during mid-fattening vs. weaning, precisely consistent with the change pattern of OFA contents as mentioned above. Based on these results, we have depicted the possible pathways implicated in the synthesis of OFAs, with acetyl-CoA and

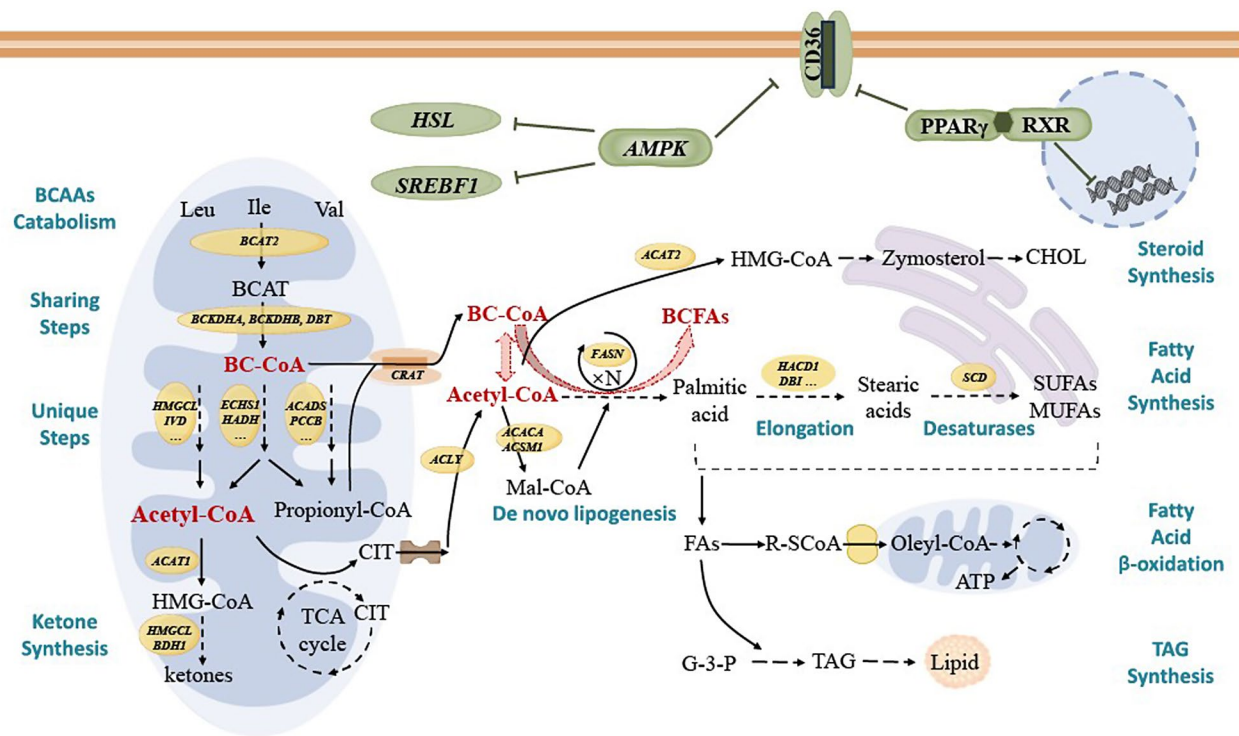


Fig. 7 Graphical representation of the mechanisms involved in lipid metabolism, branched-chain amino acid degradation pathways, and regulation of lipid metabolism in the adipose tissue of lambs. BC-CoA references to branched-chain-CoA

branched-chain-CoA intermediates as the pivotal products (Fig. 7).

Depicting the molecular regulatory mechanisms responsible for the synthesis pathways of OFAs is of utmost significance for developing nutritional manipulation strategies [37, 38]. We put this way forward to uncover that PPAR and AMPK signaling pathways might play vital roles in regulating lipid metabolism, especially OFA accumulation in the dorsal adipose tissues of lambs. On one hand, as an indispensable regulator, activation of PPAR pathway would lead to significantly differential expression of its target genes, thereafter resulting in different fat deposition patterns of two fat-tailed sheep breeds [38]. It has been reported that some of the target genes are involved in fatty acid transport (*FABP3* and *DBI*), fatty acid synthesis (*ACACA*, *SCD*), and OFA synthesis (*FASN*, *ACSF2*) in the pigs and sheep [33, 39, 40]. On the other hand, AMPK inhibits activation of the critical transcription factor *SREBF1* by phosphorylation, which stimulates fatty acid synthesis by activating key genes (*ACACA*, *LIPE*, and *FASN*) [41]. YJ Choi, KY Lee, SH Jung, HS Kim, G Shim, MG Kim, YK Oh, SH Oh, DW Jun and BH Lee [42] claimed that AMPK could enhance fatty acid uptake and lipid deposition by up-regulating expression of *CD36* in the liver of mice. Similarly, although expression of *AMPK* remained stable, we observed a drastic surge in expression of *SREBF1*, *LIPE*, and *CD36* in the adipose tissues of lambs from weaning

to market. Herein, it is reasonable to speculate that the PPAR and AMPK signaling pathways have the potential to regulate the OFA accumulation from the aspects of fatty acid synthesis and transport in lambs.

Conclusion

In the present study, we provide a comprehensive description of the dynamic accumulation of OFAs and transcriptional profiles in adipose tissue of lambs from birth to market. Our findings identify the mid-fattening vs. weaning stage as a critical time window, during which the significant surge of *de novo* lipogenesis and BCAA-degrading genes under the regulation of the PPAR and AMPK pathways contributes to the substantial synthesis and accumulation of OFAs. These findings provide novel insights into the biological processes in adipose tissue development, and offer a routine for nutritional strategies to inhibit OFA accumulation.

Abbreviations

- BCFAs Branched-chain fatty acids
- MOA 4-methyloctanoic acid
- EOA 4-ethyl-octanoic acid
- MNA 4-methylnonanoic acid
- OFAs Odor fatty acids
- DEGs Differentially expressed genes
- BCAAs Branched-chain amino acids
- FPKM Fragments per kilobase transcript length per million mapped reads
- WGCNA Weighted gene co-expression network analysis

Supplementary Information

The online version contains supplementary material available at <https://doi.org/10.1186/s12864-024-11161-w>.

Supplementary Material 1

Acknowledgements

Not applicable.

Author contributions

J.J. and Z.Y. designed the experiments, J.J., Z.Y., L.Z., O.H. and T.Z. contributed to data analysis, Z.Y. wrote the manuscript, J.J. and T.Z. significantly contributed on writing the manuscript. All authors reviewed the manuscript.

Funding

This study was supported by the International Partnership Program of Chinese Academy of Sciences (161343KYSB20200015), Training Program for Excellent Young Innovators of Changsha (kq2107011), Youth Innovation Promotion Association CAS (2023382), and the Science and Technology Innovation Program of Hunan Province (2022RC1158).

Data availability

The datasets analysed during the current study are available in the Genome Sequence Archive in National Genomics Data Center (<https://ngdc.cncb.ac.cn/gsa>), with the accession codes CRA017702.

Declarations

Ethics approval and consent to participate

The study was approved by the Animal Care and Use Committee, Institute of Subtropical Agriculture, Chinese Academy of Sciences, Changsha, China, with approval number ISA2021008. All lambs considered in this study are owned by the Institute of Subtropical Agriculture, Chinese Academy of Sciences, and informed consent has been obtained from the owner.

Consent for publication

Not applicable.

Competing interests

The authors declare no competing interests.

Received: 5 July 2024 / Accepted: 16 December 2024

Published online: 31 December 2024

References

- Godfray HCJ, Aveyard P, Garnett T, Hall JW, Key TJ, Lorimer J, Pierrehumbert RT, Scarborough P, Springmann M, Jebb SA. Meat consumption, health, and the environment. *Science*. 2018; 361(6399).
- Cabrera MC, Saadoun A. An overview of the nutritional value of beef and lamb meat from South America. *Meat Sci.* 2014;98(3):435–44.
- Payne CE, Pannier L, Anderson F, Pethick DW, Gardner GE. Lamb age has little impact on eating quality. *Foods* 2020, 9(2).
- O'Reilly RA, Pannier L, Gardner GE, Garmyn AJ, Luo H, Meng Q, Miller MF, Pethick DW. Minor differences in perceived sheepmeat eating quality scores of Australian, Chinese and American consumers. *Meat Sci.* 2020;164:108060.
- Miller R. Drivers of consumer liking for beef, pork, and lamb: a review. *Foods* 2020, 9(4).
- Wu T, Wang P, Zhang Y, Zhan P, Zhao Y, Tian H, He W. Identification of muttoney-related compounds in cooked mutton tallows and their flavor intensities subjected to phenolic extract from thyme (*Thymus vulgaris* L). *Food Chem.* 2023;427:136666.
- Kaffarnik S, Preuss S, Vetter W. Direct determination of flavor relevant and further branched-chain fatty acids from sheep subcutaneous adipose tissue by gas chromatography with mass spectrometry. *J Chromatogr A.* 2014;1350:92–101.
- Watkins PJ, Rose G, Salvatore L, Allen D, Tucman D, Warner RD, Dunshea FR, Pethick DW. Age and nutrition influence the concentrations of three branched chain fatty acids in sheep fat from Australian abattoirs. *Meat Sci.* 2010;86(3):594–9.
- Gravador RS, Harrison SM, Monahan FJ, Gkarane V, Farmer LJ, Brunton NP. Validation of a rapid microwave-assisted extraction method and gc-fid quantification of total branched chain fatty acids in lamb subcutaneous adipose tissue. *J Food Sci.* 2019;84(1):80–5.
- Jiao J, Wu J, Zhou C, He Z, Tan Z, Wang M. Ecological niches and assembly dynamics of diverse microbial consortia in the gastrointestinal of goat kids. *ISME J.*; 2024.
- Zhang B, Sun Z, Yu Z, Li H, Luo H, Wang B. Transcriptome and targeted metabolome analysis provide insights into bile acids' new roles and mechanisms on fat deposition and meat quality in lamb. *Food Res Int.* 2022;162(Pt A):111941.
- Zhao X, Zuo S, Guo Y, Zhang C, Wang Y, Peng S, Liu M, Wang B, Zhang H, Luo H. Carcass meat quality, volatile compound profile, and gene expression in Tan sheep under different feeding regimes. *Food Biosci* 2023, 56:103213.
- Zhang X, Wu J, Zhou C, Wang M, Tan Z, Jiao J. Temporal changes in muscle characteristics during growth in the goat. *Meat Sci.* 2023;200:109145.
- Wallace M, Green CR, Roberts LS, Lee YM, McCarville JL, Sanchez-Gurmaches J, Meurs N, Gengatharan JM, Hover JD, Phillips SA, et al. Enzyme promiscuity drives branched-chain fatty acid synthesis in adipose tissues. *Nat Chem Biol.* 2018;14(11):1021–31.
- Li J, Zhang D, Yin L, Li Z, Yu C, Du H, Jiang X, Yang C, Liu Y. Integration analysis of metabolome and transcriptome profiles revealed the age-dependent dynamic change in chicken meat. *Food Res Int.* 2022;156:111171.
- Hewavitharana GG, Perera DN, Navaratne SB, Wickramasinghe I. Extraction methods of fat from food samples and preparation of fatty acid methyl esters for gas chromatography: a review. *Arab J Chem.* 2020;13(8):6865–75.
- Jiao J, Zhang X, Wang M, Zhou C, Yan Q, Tan Z. Linkages between epithelial microbiota and Host Transcriptome in the Ileum during High-Grain challenges: implications for gut homeostasis in goats. *J Agric Food Chem.* 2019;67(1):551–61.
- Li R, Li Y, Kristiansen K, Wang J. SOAP: short oligonucleotide alignment program. *Bioinformatics.* 2008;24(5):713–4.
- Kim D, Langmead B, Salzberg SL. HISAT: a fast spliced aligner with low memory requirements. *Nat Methods.* 2015;12(4):357–60.
- Langmead B, Salzberg SL. Fast gapped-read alignment with Bowtie 2. *Nat Methods.* 2012;9(4):357–9.
- Li B, Dewey CN. RSEM: accurate transcript quantification from RNA-Seq data with or without a reference genome. *BMC Bioinf.* 2011;12:323.
- Storey JD. False Discovery Rate. In: *International Encyclopedia of Statistical Science*. Edited by Lovric M. Berlin, Heidelberg: Springer Berlin Heidelberg; 2011: 504–508.
- Langfelder P, Horvath S. WGCNA: an R package for weighted correlation network analysis. *BMC Bioinf.* 2008;9:559.
- Resconi V, Escudero A, Campo M. The development of aromas in ruminant meat. *Molecules.* 2013;18(6):6748–81.
- Tchkonina T, Thomou T, Zhu Y, Karagiannides I, Pothoulakis C, Jensen MD, Kirkland JL. Mechanisms and metabolic implications of regional differences among fat depots. *Cell Metab.* 2013;17(5):644–56.
- Gravador RS, Moloney AP, Brunton NP, Gkarane V, Allen P, Fahey AG, Claffey NA, Diskin MG, Farmer LJ, Monahan FJ. Effects of castration and slaughter age on the fatty acid composition of ovine muscle and adipose tissue from two breeds. *Small Ruminant Res.* 2018;168:94–100.
- Fainberg HP, Birtwistle M, Alagal R, Alhaddad A, Pope M, Davies G, Woods R, Castellanos M, May ST, Ortori CA, et al. Transcriptional analysis of adipose tissue during development reveals depot-specific responsiveness to maternal dietary supplementation. *Sci Rep.* 2018;8(1):9628.
- Yuan Y, Sun DM, Qin T, Mao SY, Zhu WY, Yin YY, Huang J, Heller R, Li ZP, Liu JH, et al. Single-cell transcriptomic landscape of the sheep rumen provides insights into physiological programming development and adaptation of digestive strategies. *Zool Res.* 2022;43(4):634–47.
- Wang H, Zhong J, Zhang C, Chai Z, Cao H, Wang J, Zhu J, Wang J, Ji Q. The whole-transcriptome landscape of muscle and adipose tissues reveals the ceRNA regulation network related to intramuscular fat deposition in yak. *BMC Genomics.* 2020;21(1):347.
- Lu H, Wang Z, Cao B, Cong F, Wang X, Wei W. Dietary sources of branched-chain fatty acids and their biosynthesis, distribution, and nutritional properties. *Food Chem* 2024, 431:137158.
- Pietrocola F, Galluzzi L, Bravo-San Pedro JM, Madeo F, Kroemer G. Acetyl coenzyme A: a central metabolite and second messenger. *Cell Metab.* 2015;21(6):805–21.

32. Heil CS, Wehrheim SS, Paithankar KS, Grninger M. Fatty acid biosynthesis: chain-length regulation and control. *ChemBioChem*. 2019;20(18):2298–321.
33. Dervishi E, Serrano C, Joy M, Serrano M, Rodellar C, Calvo JH. The effect of feeding system in the expression of genes related with fat metabolism in semitendinous muscle in sheep. *Meat Sci*. 2011;89(1):91–7.
34. Fassah DM, Kang HJ, Beak SH, Jung DJS, Jeong I, Na SW, Yoo SP, Hong SJ, Kim HJ, Haque MN, et al. Effects of dietary glycerol supplementation on meat quality, palatability, and lipid metabolism gene expression in the longissimus thoracis of Hanwoo steers. *Meat Sci*. 2023;198:109093.
35. Green CR, Wallace M, Divakaruni AS, Phillips SA, Murphy AN, Ciaraldi TP, Metallo CM. Branched-chain amino acid catabolism fuels adipocyte differentiation and lipogenesis. *Nat Chem Biol*. 2016;12(1):15–21.
36. Arany Z, Neinast M. Branched chain amino acids in metabolic disease. *Curr Diabetes Rep*. 2018;18(10):76.
37. Gunawan A, Jakaria, Listyarini K, Furqon A, Sumantri C, Akter SH, Uddin MJ. Transcriptome signature of liver tissue with divergent mutton odour and flavour using RNA deep sequencing. *Gene*. 2018;676:86–94.
38. Li B, Qiao L, An L, Wang W, Liu J, Ren Y, Pan Y, Jing J, Liu W. Transcriptome analysis of adipose tissues from two fat-tailed sheep breeds reveals key genes involved in fat deposition. *BMC Genomics*. 2018;19(1):338.
39. Zhang L, Li F, Guo Q, Duan Y, Wang W, Yang Y, Yin Y, Gong S, Han M, Yin Y. Different proportions of branched-chain amino acids modulate lipid metabolism in a finishing pig model. *J Agric Food Chem*. 2021;69(25):7037–48.
40. Zhao Y, Zhang Y, Khas E, Bai C, Cao Q, Ao C. Transcriptome analysis reveals candidate genes of the synthesis of branched-chain fatty acids related to mutton flavor in the lamb liver using *Allium Mongolicum* Regel extract. *J Anim Sci* 2022, 100(9).
41. Bordoloi J, Ozah D, Bora T, Kalita J, Manna P. Gamma-Glutamyl carboxylated Gas6 mediates the beneficial effect of vitamin K on lowering hyperlipidemia via regulating the AMPK/SREBP1/PPAR α signaling cascade of lipid metabolism. *J Nutr Biochem*. 2019;70:174–84.
42. Choi YJ, Lee KY, Jung SH, Kim HS, Shim G, Kim MG, Oh YK, Oh SH, Jun DW, Lee BH. Activation of AMPK by berberine induces hepatic lipid accumulation by upregulation of fatty acid translocase CD36 in mice. *Toxicol Appl Pharmacol*. 2017;316:74–82.

Publisher's note

Springer Nature remains neutral with regard to jurisdictional claims in published maps and institutional affiliations.